

Light Microscopic Analysis of the Intrinsic Properties of Magnetically Hard Phases from the Domain Structure

Light Microscopic Analysis of the Intrinsic Properties of Magnetically Hard Phases from the Domain Structure

Authors: Ralf Löffler, Dagmar Goll, Gerlinde Guth,
Timo Bernthaler, Gerhard Schneider
Aalen University, Materials Research Institute

Volker Pusch
Carl Zeiss Microscopy GmbH

Date: March 2016

Magnetically hard materials have a large coercive field H_c , a high degree of remanence J_R , and a high maximum energy product $(BH)_{\max}$. Remanence is essentially determined by saturation magnetic polarization J_s and the coercive field of magnetocrystalline anisotropy K_1 . Magnets from rare earth metals and transition metals currently achieve the highest energy products, such as $\text{Nd}_2\text{Fe}_{14}\text{B}$, with 450 kJ/m^3 [1]. High demand and dependence on raw materials are leading to a highly intensified search for new magnetically hard phases with reduced selenium content.

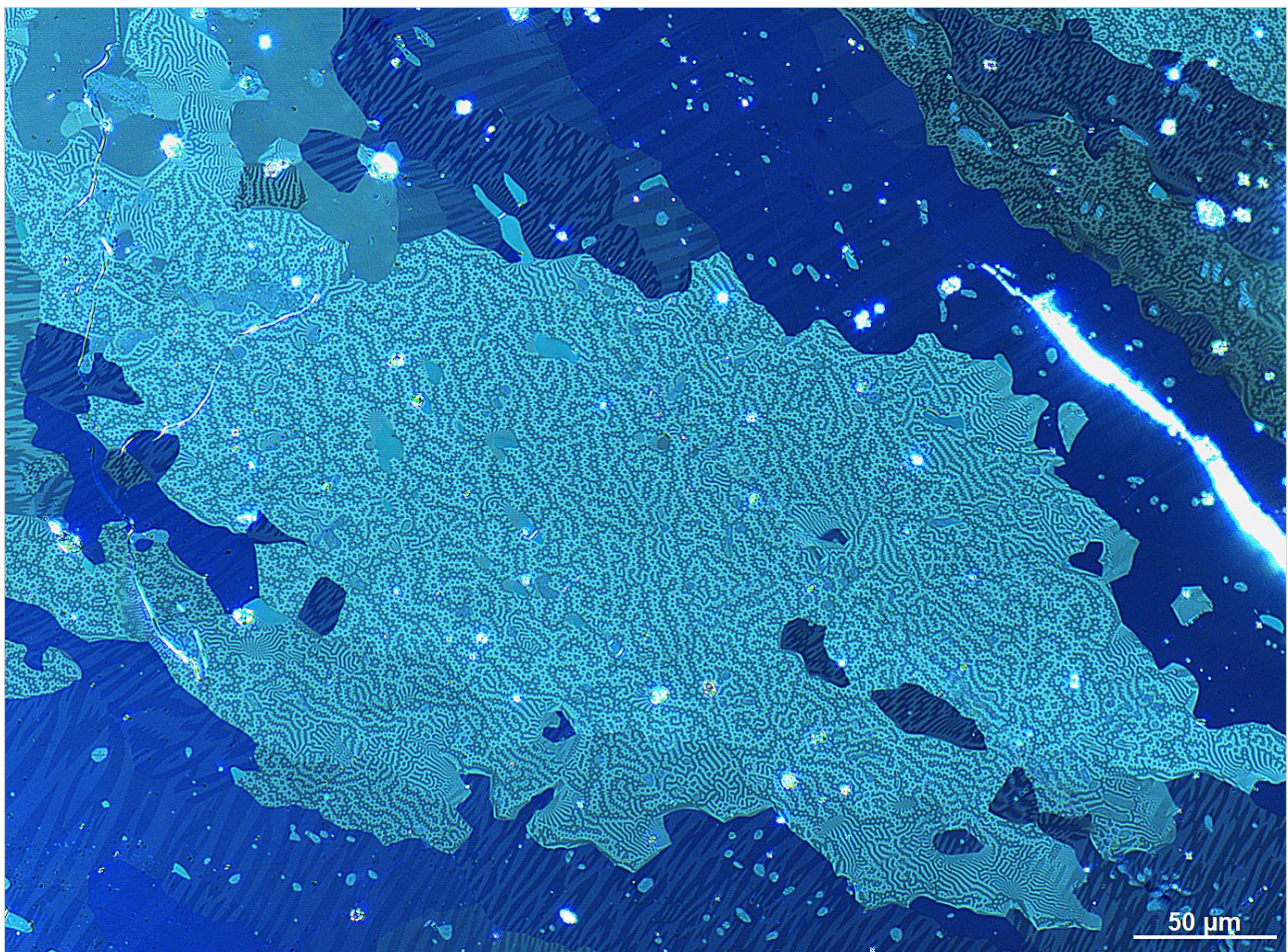


Figure 1: Kerr image of an $\text{Nd}_2\text{Fe}_{14}\text{B}$ smelting sample at 200x magnification in a compound microscope with typical and in some cases complex domain patterns (closure domains: turquoise; stripe domains: dark blue).

Introduction

In addition to the classic method of determining the magnetic characteristics H_c , J_R , and $(BH)_{\max}$ from hysteresis, the intrinsic magnetic properties J_s and K_1 can be determined from the domain pattern. The magnetic domains are visualized on polished surfaces of materialographic preparations using, for example, the magneto-optic Kerr effect [2] (figures 1 and 2). To utilize the Kerr effect, the polished surface of a magnetic specimen is illuminated with linear polarized light. Due to the sample's magnetic stray field, the polarization plane of the observed reflected light beam is then slightly rotated or is typically polarized elliptically. If one views the resulting reflected light through an analyzer, the domains appear at different levels of brightness with a different orientation to the spontaneous polarization. The difference in brightness (= domain contrast) is a measure of the saturation magnetic polarization J_s and the domain width is a measure of the anisotropy constant K_1 . For iron-rich, ferromagnetic phases, an approximately linear relationship is measured between magnetization and the Kerr rotation angle [3], and by means of this to domain contrast in the Kerr image. Wall energy γ , and by way of this, the anisotropy constant K_1 , can be calculated for single-axis magnetic phases from the measured width of the stripe domains [3, 4, 5, 6] or the closure domains [7, 8] using different mathematical models.

It is possible to observe the Kerr effect with special Kerr microscopes and with laser scanning as well as compound light microscopes. Using the approach of sensory microscopy, the goal is to develop and verify a method which can be used to directly calculate the intrinsic, hard-magnetic properties using a classic compound microscope and digital image analysis from the domain structure.

Experiment

Samples used: The experiment was carried out using five iron-rich, magnetically hard phases: $\text{Nd}_2\text{Fe}_{14}\text{B}$, $\text{Pr}_2\text{Fe}_{14}\text{B}$, $\text{Y}_2\text{Fe}_{14}\text{B}$, $\text{Ce}_2\text{Fe}_{14}\text{B}$, $\text{BaFe}_{12}\text{O}_{19}$ (hexaferrite), and SmCo_5 . The first four samples were produced in an electric arc furnace as stoichiometric smelting samples. Hexaferrite is a commercial product. These magnetically hard phases are extremely well studied in scientific literature and, as such, are suited for correlating the intrinsic hard-magnetic properties with the quantitative results of the evaluated domain images (Figure 3). The polished surface of materialographic preparations were produced using classic preparation techniques. A particular emphasis was placed on an artifact-free specimen surface.

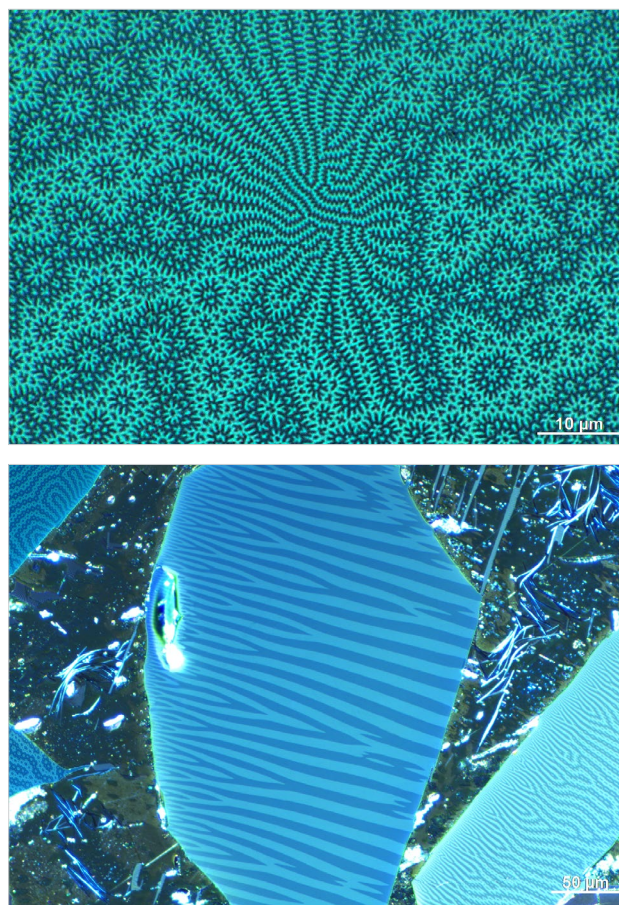


Figure 2, top: Kerr image of an $\text{Nd}_2\text{Fe}_{14}\text{B}$ closure domain at 1000x magnification in the compound microscope. The domain pattern in the center of the image is typical for a lesser grain thickness (such as a pore directly below the specimen surface).

Bottom: Stripe domain pattern at 200x magnification of $\text{Nd}_2\text{Fe}_{14}\text{B}$. The branching out of the stripes in the direction of the surface is typical for single-axis magnetic phases with a high level of crystal anisotropy.

Hardware, image acquisition, and the experimental program: The Kerr analyses were conducted using a fully automated Axio Imager.Z2m compound microscope in linearly polarized light. The microscope was controlled using AxioVision. The imaging of the domains was created using the objective lenses EC Epiplan-NEOFLUAR 50x/0.80 and 100x/1.3 Oil Pol. HXP 120 C with light guide was used as the light source to illuminate the image in a homogeneous manner. Standard image acquisition was carried out with AxioCam HRC microscope camera for the best possible ranges of contrast. For the respective objectives, special shading corrections were created which were carefully crafted specifically for polarization microscopy. To determine the ideal exposure time for each domain, a small frame of measurement was used within the domains, in which the microscope was then focused and the exposure time subsequently determined automatically. In the event of microtopo-

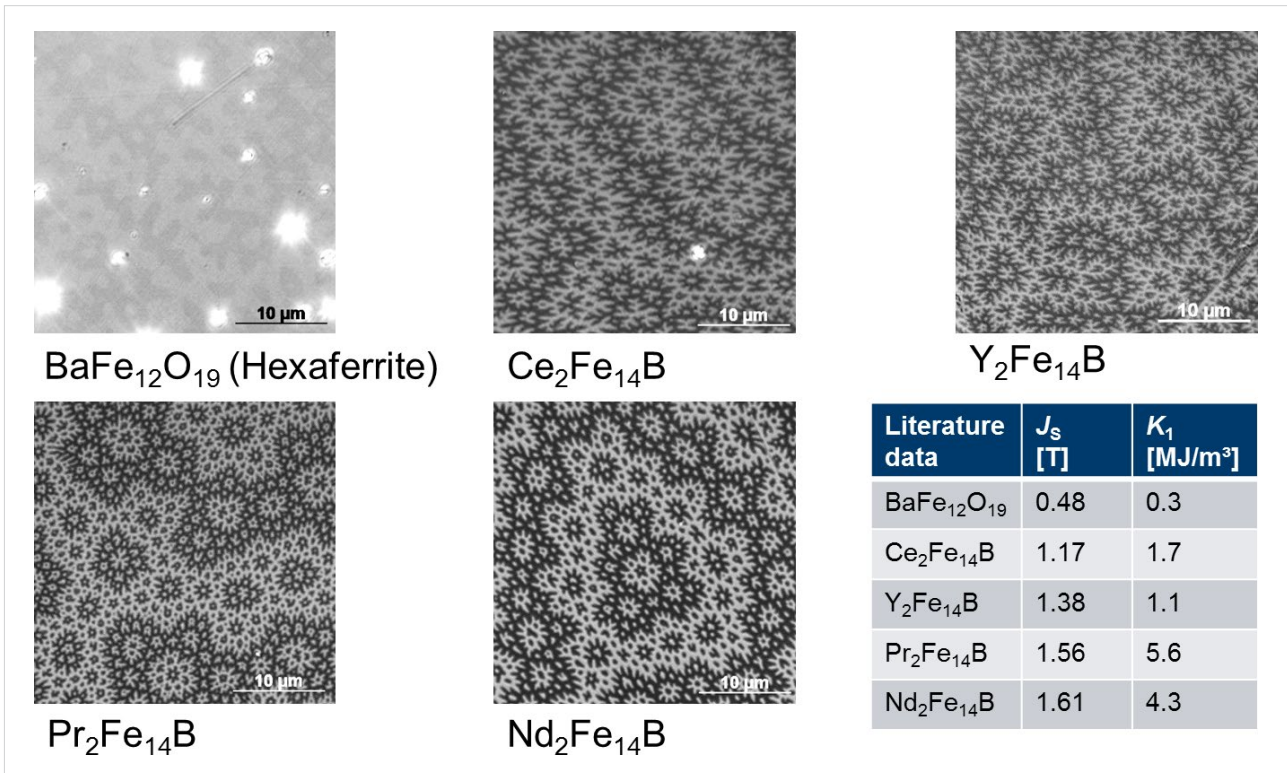


Figure 3: Exemplary image sections of the closure domains of the analyzed hard-magnetic phases at 1000x magnification. From a qualitative standpoint, differences are apparent in both domain width and contrast.

graphies, a uniformly focused image was created using extended depth of field where necessary. Quantitative determination of domain contrast: The domain contrast of closure domains was carried out using eight-bit grayscale images and was evaluated in defined areas from the center of the acquired domain image. Doing so eliminated a distortion of the results due to any

shading effects which may have been present. The quantitative determination of domain contrast was carried out in AxiVision through (A) the calculation of peak values on the histogram as well as (B) by image analysis-based calculation of the median gray value around both maxima using threshold segmentation (Figure 4a). Quantitative determination of the

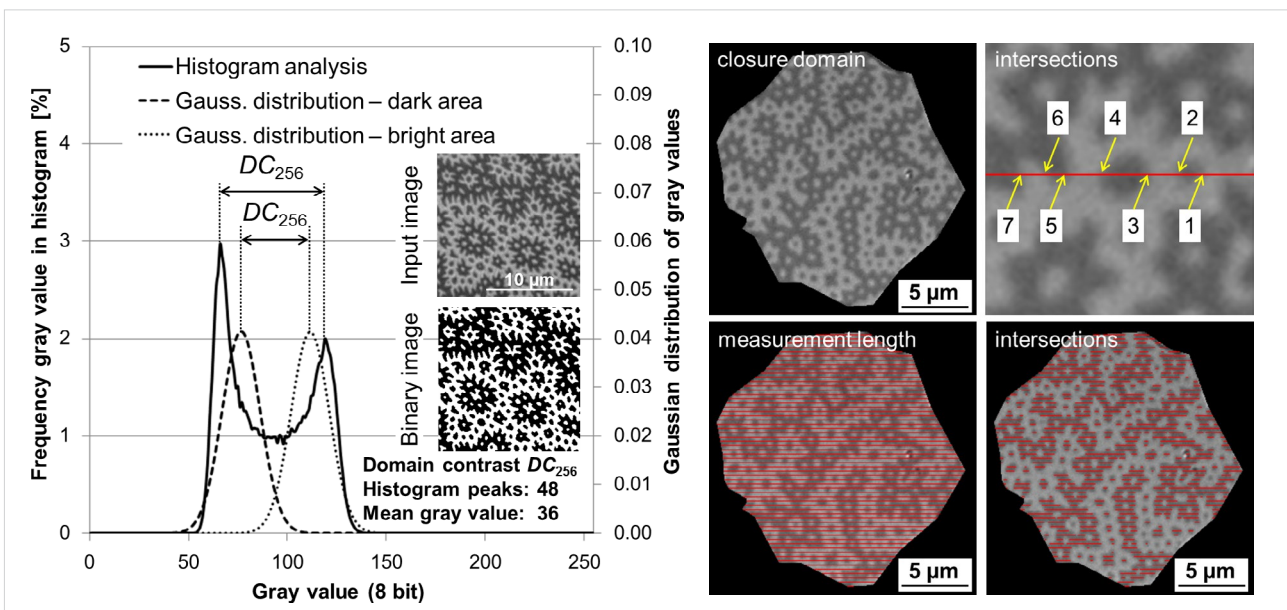


Figure 4: a) Method for quantitative calculation of domain contrast and b) of domain surface width using image analysis.

domain width using $\text{Nd}_2\text{Fe}_{14}\text{B}$ as an example: The calculation of the median domain width D_s of closure domains was carried out using the stereological approach of the linear intercept method as set forth in [8], similar to how it is used in the classic particle size analysis of steel. The image analysis-based calculation of the intercept points and the entire measured section was achieved using an adjusted automated vertical and horizontal linear analysis in AxioVision (Figure 4b). Domain width D_m and particle size L were measured interactively in AxioVision on suitable stripe domains. The median value for D_m and L were then determined subsequently for each particle.

Results

The quantitatively calculated domain contrasts of the analyzed iron-rich hard-magnetic phases correlate extremely well with the saturation polarization J_s of the respective phase. For example, hexaferrite, which has the lowest level of saturation magnetic polarization, also exhibits the by far least amount of domain contrast, while $\text{Nd}_2\text{Fe}_{14}\text{B}$, with the highest level of saturation magnetic polarization, exhibits the largest amount of domain contrast.

The domain contrasts of the other three hard-magnetic phases lie between hexaferrite and $\text{Nd}_2\text{Fe}_{14}\text{B}$ based on their saturation magnetic polarization (Figure 5).

The contrasts of the Co-Sm phases do not lie on the line of the phases containing Fe, however. Further examination is required to determine the reasons for this.

For $\text{Nd}_2\text{Fe}_{14}\text{B}$, a median domain surface width D_s gives results with a value of $0.57 \pm 0.13 \mu\text{m}$. Using the model set forth in [9] and the values from the literature for saturation magnetization and the exchange constant, the anisotropy constant K_1 is calculated as 4.6 MJ/m^3 . This corresponds extremely well with the value from the literature of $K_1 = 4.3 \text{ MJ/m}^3$. For stripe domains, the anisotropy constant K_1 is calculated as 4.8 MJ/m^3 using the model set forth in [6]. For particle sizes where $L > 10 \mu\text{m}$, this model provides values which correspond best with the values from the literature.

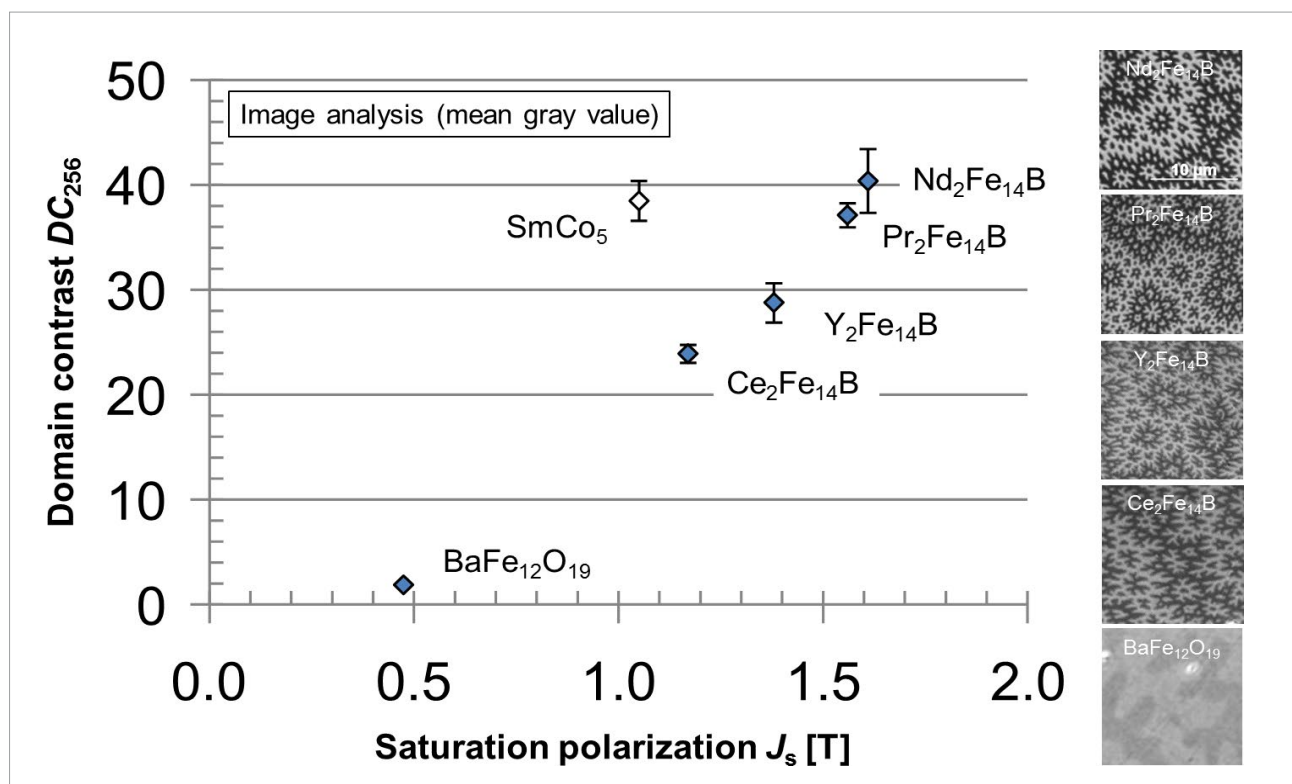


Figure 5: Correlation of the quantitatively determined domain contrasts with the saturation magnetic polarization of the analyzed hard-magnetic phases.

Summary

The approach of sensory microscopy on a carefully configured compound microscope is a resource-efficient method which can be used to directly derive the intrinsic properties of the analyzed hard-magnetic phases from the micrograph.

The core in this context is the quantification of the domain structure through image analysis with regard to its contrast and median width. For iron-rich, hard-magnetic phases, the domain contrasts can be used to evaluate the saturation magnetic polarization J_s . The anisotropy constant K_1 can be calculated with a high level of accuracy using the median domain width determined through image analysis in conjunction with mathematical models. This opens up new prospects in magnetic research and quality assurance. For example, new hard-magnetic phases can be evaluated quickly with regard to their potential areas of application.

Literature

- [1] W. Rodewald, in Handbook of magnetism and advanced magnetic materials (eds. H. Kronmüller, S. Parkin), John Wiley & Sons, 1969–2004 (2007)
- [2] H.J. Williams, F.G. Foster, E.A. Wood, Phys. Rev. **82**, 119–120 (1951)
- [3] K.H.J. Buschow, P.G. van Engen, R. Jongebreur, J. Magn. Magn. Mater. **38**, 1–22 (1983)
- [4] C. Kittel, Phys. Rev. **70**, 965 (1946)
- [5] J. Kaczer, Sov. Phys. JETP **19**, 1204 (1964)a
- [6] R. Szymczak, Acta Phys. Pol. A **43**, 571 (1973)
- [7] A. Hubert, Phys. Stat. Sol. **24**, 669 (1967)
- [8] R. Bodenberger, A. Hubert, Phys. Stat. Sol. (a) **44**, K7–K11 (1977)



Carl Zeiss Microscopy GmbH
07745 Jena, Germany
microscopy@zeiss.com
www.zeiss.com/microscopy



Not for therapeutic, treatment or medical diagnostic evidence. Not all products are available in every country. Contact your local ZEISS representative for more information.

EN_42_011_030 | CZ 03-2016 | Design, scope of delivery, and technical progress subject to change without notice. | © Carl Zeiss Microscopy GmbH